Reverse Microemulsion-Mediated Synthesis of SiO_2-Coated ZnO Composite Nanoparticles: Multiple Cores with Tunable Shell Thickness

Jinfeng Wang, Takuya Tsuzuki, Lu Sun,* and Xungai Wang

Centre for Material and Fibre Innovation, Institute for Technology Research and Innovation, Deakin University, Geelong, Victoria 3217, Australia

ABSTRACT Monodispersed SiO_2-shell/ZnO-core composite nanospheres have been prepared in an oil-in-water microemulsion system. By using cyclohexane as the oil phase and Triton X-100 as the surfactant, composite nanospheres with high core loading levels and tunable shell thickness were obtained. Utilization of PVP capping agent on ZnO allowed the synthesis of composite nanospheres without forming any coreless SiO_2 spheres or shell-less ZnO particles. The photoactivity of ZnO nanoparticles was greatly reduced by SiO_2-coating, which enables their applications as durable, safe, and nonreactive UV blockers in plastics, coating, and other products.

KEYWORDS: reverse microemulsion • photocatalytic activity • core/shell nanoparticles • ZnO • SiO_2

INTRODUCTION

SiO_2-based composite nanospheres are of particular interest to many applications because of their biocompatibity, chemical stability, and ease of surface modification with a wide range of functional groups. By incorporating other types of materials, such as quantum dots (1) or magnetic nanoparticles (2–4), the composite nanospheres can become multifunctionalized. However, a common problem of SiO_2-based composite nanospheres that are multifunctionalized by core materials is that only a relatively limited degree of the new functionality is realized because of the low loading levels of core nanoparticles (2). To increase the functionality that arises from the incorporated nanoparticles in the SiO_2 spheres, it is of interest to achieve high loading levels of nanoparticles in each SiO_2 sphere. To date, only a limited number of studies have reported that high loading levels of functional materials were incorporated in SiO_2 spheres (5), especially for small particles, i.e., ~50 nm (1, 6).

Nanosized zinc oxide (ZnO) has attracted increasing attention as one of the multifunctional inorganic nanoparticles because of its promising applications in solar cells (7), electronic devices (8), ultraviolet (UV)-light detectors (9), photodiodes (10), and catalysis (11). ZnO has also been widely used as an excellent UV absorber in outdoor textiles and personal-care products (12, 13). However, the application of ZnO as an UV absorber is limited in many practical areas because of the inherent photocatalytic activity of ZnO which results in color fading of fabrics (14) and potential damage of the skin cells (15). It is expected that fabrication of a SiO_2-shell around ZnO nanoparticles would reduce the photocatalytic activity, because of the entrapment of photogenerated electrons and holes inside of the SiO_2 shell. Multiple ZnO core in those composite nanospheres is advantageous for high UV screening efficacy.

In this work, we demonstrated the preparation of monodispersed ZnO-core/SiO_2-shell core−shell-structured nanospheres with high core loading levels, using a modified microemulsion method. Although the reverse microemulsion technique had been used in the past to apply SiO_2 coatings on II−IV semiconductor quantum dots (6), gold and silver nanoparticles (16), and magnetic iron oxide nanoparticles (2, 17), to the best of our knowledge, this is the first time the technique has been successfully applied to ZnO to form ZnO-core/SiO_2-shell composite nanoparticles.

EXPERIMENTAL SECTION

First, hydrophilic PVP-capped ZnO nanoparticles were synthesized separately according to a previous report (18). A reverse microemulsion system was prepared separately by sonicating the mixture of polyethylene glycol octylphenyl ether (1.77 g Triton X-100) and *n*-hexanol (1.8 mL) in cyclohexane (7.5 mL). Next, 480 μL of PVP−ZnO dispersion (2 mM water) was added to the reverse microemulsion medium. After NH_4OH (29.4% 60 μL) was added to the mixture, the medium was stirred to make uniform emulsion system. Finally tetraethyl orthosilicate (TEOS, 100 μL, Aldrich) was mixed in the system. The mixture was aged for different durations up to 48 h. The resulting SiO_2-coated ZnO composite nanoparticles were collected by centrifuging, followed by washing and redispersion in ethanol or deionized water. The whole process was carried out at room temperature.

X-ray diffraction (XRD) data were obtained on a Phillips PW-1729 Diffractometer (35 kV, 28 mA) with Cu-kα radiation at a scanning rate of 2.4° min^{-1}. The morphologies and structures of the samples were investigated by transmission

* To whom correspondence should be addressed. E-mail: lu.sun@deakin.edu.au.

Received for review January 18, 2010 and accepted March 15, 2010

DOI: 10.1021/am100051z

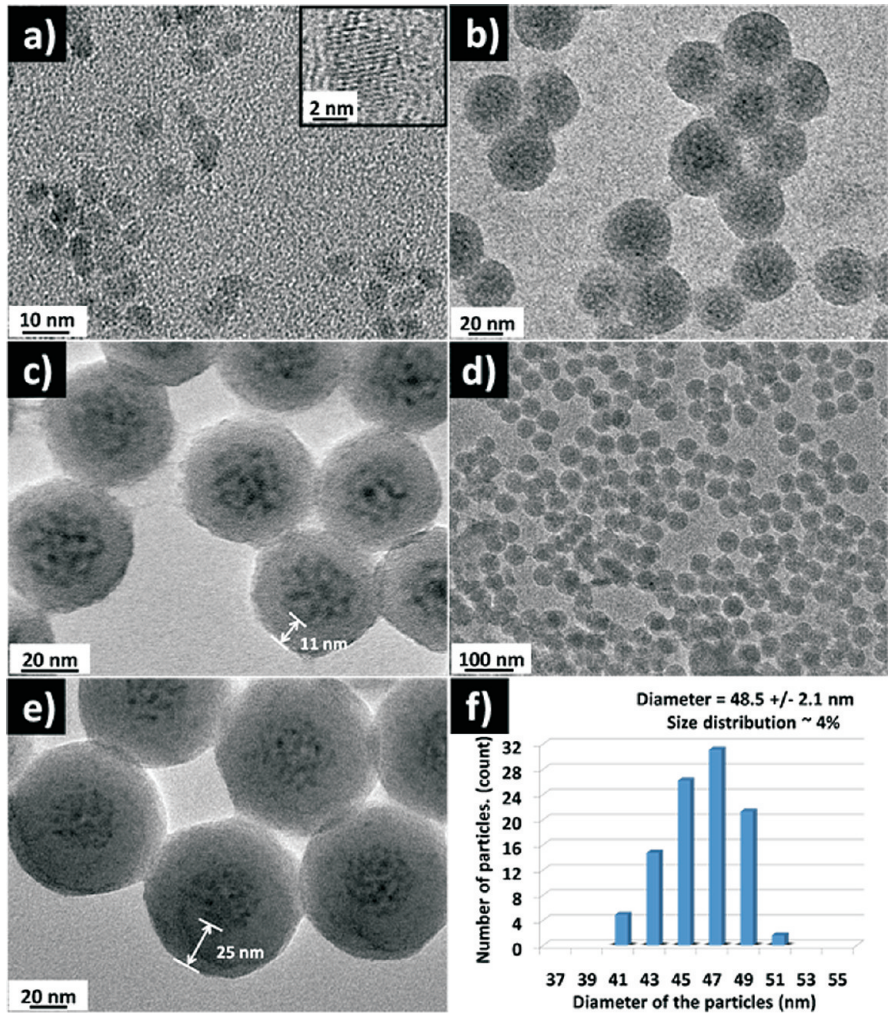

FIGURE 1. (a) TEM micrograph of PVP-capped ZnO nanoparticles. Inset is a high-resolution image of a particle. (b–e) TEM micrographs of ZnO-core/SiO_2-shell composite nanoparticles prepared with different reaction times of (b) 8, (c, d) 24, and (e) 48 h. (f) Size distribution of ZnO-core/SiO_2-shell composite nanoparticles after 24 h of reaction time.

electron microscopy (TEM) on a JEM-2100 with an acceleration voltage of 200 kV. The optical absorption spectra of the samples were obtained using a Varian Cary 3E UV/vis spectrophotometer. In the photocatalytic activity test, Rhodamine B (RhB) was used as a probe molecule to evaluate the photocatalytic activity of PVP-capped ZnO and ZnO-core/SiO_2-shell composite nanoparticles in respond to UV and visible light irradiation.

RESULTS AND DISCUSSION

A typical TEM image of the uncoated PVP-capped ZnO nanoparticles is shown in Figure 1a. The nanoparticles were monodispersed and single-crystalline. TEM image analysis revealed that the average diameter was 4.6 nm and the size distribution was ~85%. UV/vis spectroscopy showed that the optical absorption wavelength associated with the band-gap energy shifted to a lower value than that of bulk ZnO (375 nm) (19), indicative of a quantum confinement effect (Figure 2b). XRD spectra confirmed that the ZnO nanoparticles had the wurtzite-type crystal structure (Figure 2a). After hydrolysis and condensation of TEOS in the microemulsions for 12 h, a mixture of primary particles and large particles (24–50 nm) that approached a spherical morphology was observed (Figure 1b). After 24 h of reaction time, only highly monodispersed spherical particles were formed (Figure 1c), where a SiO_2 shell was developed around the core that consisted of many ZnO nanoparticles (Figure 1d). All the ZnO nanoparticles in the core appeared individually dispersed in the SiO_2 matrix. PVP-capped ZnO nanoparticles were always in the center of the composites. The surface of the nanospheres appeared quite smooth. TEM image analysis revealed that the composite nanospheres were quite uniform in size (Figure 1d) with an average diameter of 48.5 ± 2.1 nm and a size distribution of ~4% (Figure 1f). No coreless SiO_2 spheres or shell-less ZnO nanoparticles were found by TEM study. As the reaction time was prolonged from 24 to 48 h, the shell thickness increased from 11 to 25 nm (Figures 1c and 1e).

To prove that the dark spots in the particles in images c and e in Figure 1 were in fact ZnO crystals, we performed XRD and UV/vis analyses. Figure 2a shows the XRD patterns of the uncoated PVP-capped ZnO and ZnO-core/SiO_2-shell composite nanoparticles. The spectra of both samples cor-

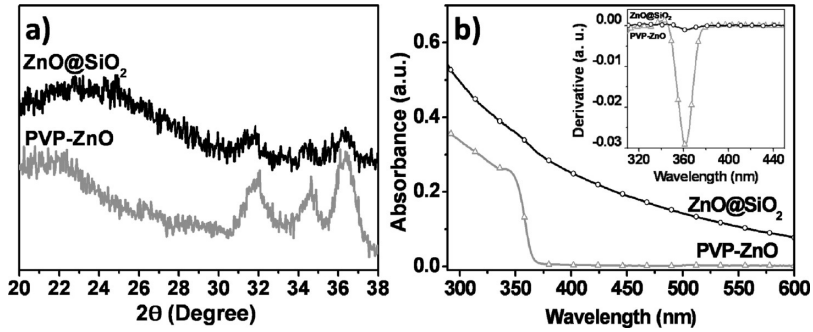

FIGURE 2. (a) Powder X-ray diffraction spectra of PVP-capped ZnO and ZnO-core/SiO_2-shell composite nanoparticles after 24 h of reaction time; (b) UV/vis absorption spectra of PVP-capped ZnO and ZnO-core/SiO_2-shell composite nanoparticle suspensions at 1 mg mL^{-1} in absolute ethanol. Inset is the derivatives of UV/vis absorption curves.

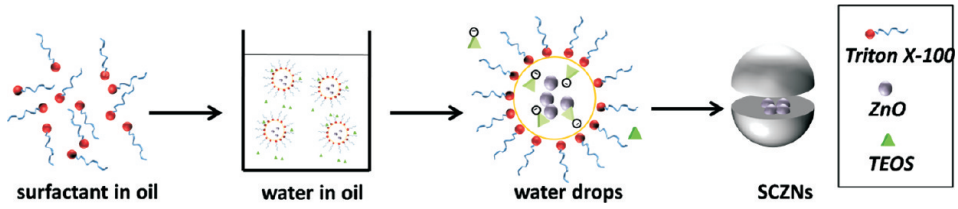

FIGURE 3. Schematic diagram of the formation mechanism of ZnO-core/SiO_2-shell composite nanoparticles via a reverse microemulsion method.

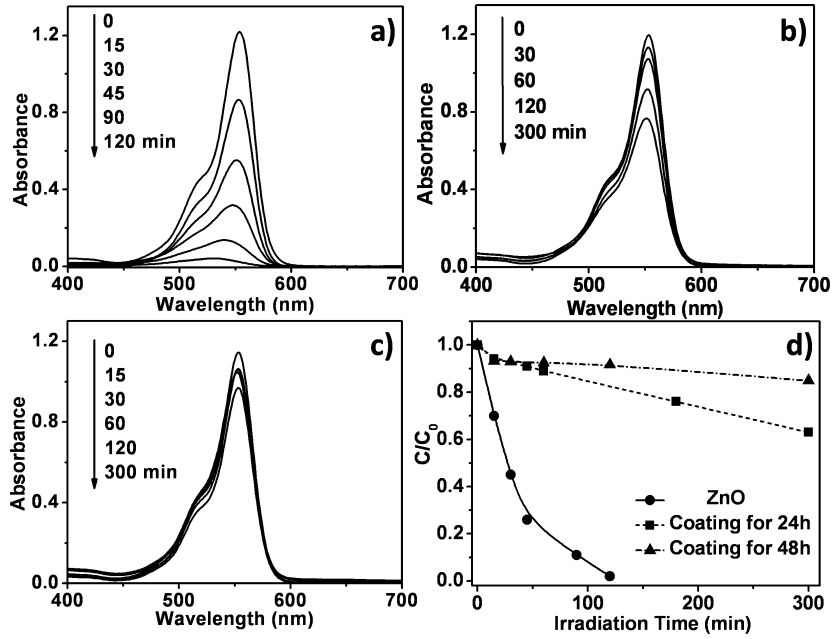

FIGURE 4. Absorption spectra of Rhodamine B solutions as a function of light irradiation time in the presence of (a) PVP-capped ZnO, (b) ZnO-core/SiO_2-shell composite nanoparticles after reaction for 24 h, and (c) after reaction for 48 h. (d) Relative change in the intensity of the absorption peak of Rhodamine B as a function of irradiation time.

related well with that of wurtzite ZnO, indicative of the presence of ZnO in the SiO_2 shell.

Figure 2b shows UV-absorbance spectra of PVP-capped ZnO and ZnO-core/SiO_2-shell composite nanoparticle suspensions. The PVP-capped ZnO sample showed a sharp absorption onset at ~365 nm that corresponds to the bandgap energy of ZnO quantum dots, which was clearly evident due to the little light scattering caused by the small particles. On the other hand, ZnO-core/SiO_2-shell composite nanoparticles did not show clear bandgap absorption due to the strong light scattering caused by the large particle size. To analyze the difference in bandgap energy between the two samples, the first derivative of the absorbance spectra, which corresponds to the inflection points of the absorption spectra, were calculated. As shown in the inset of Figure 2b, the peak positions of the first derivative were identical in both samples. This indicates that ZnO was present in the resulting nanoparticles and that the ZnO in SiO_2 shells had nearly the same bandgap energy as that of starting PVP-capped ZnO nanoparticles. The results indicate that the PVP-capped ZnO nanoparticles were successfully encapsulated in SiO_2 while remaining as quantum dots.

These observations, together with previously published works on nanocomposites through reverse microemulsion

methods (20–23), suggest that the formation mechanism can be described as follows (Figure 3): The PVP-capped ZnO nanoparticles are dispersed in water droplets in the reverse microemulsion. When TEOS is added, it is first dissolved in the oil phase, and then hydrolyzed at the water/oil interphase. As the hydrization progresses, the SiO_2 precursor is transferred into the water phase and finally forms SiO_2 coatings on the surface of the PVP-capped ZnO. Further hydrization of TEOS contributes to the increase in the shell thickness and the formation of smooth surface. This modified water-in-oil technique offers the following advantages over the conventional SiO_2 coating techniques such as the Stöber method: (1) PVP-capping agent provides ZnO nanoparticles with good dispersion stability at high particle concentration, leading to the high loading levels of PVP-capped ZnO in the final composite nanoparticles; (2) PVP-capping increases their affinity of ZnO surface toward SiO_2 (24), which avoids the formation of core-less SiO_2 spheres and shell-less ZnO; and (3) NH_4OH is constrained in the water droplets together with ZnO nanoparticles, which ensures that the hydrolysis and condensation reactions occur only in the water droplets in the presence of ZnO, which again avoids the formation of coreless SiO_2 spheres and shell-less ZnO.

Figure 4 shows the time-dependent absorption spectra of RhB aqueous solutions during the UV light irradiation in the presence of PVP-capped ZnO and ZnO-core/SiO_2-shell composite nanoparticles with different shell thicknesses. For PVP-capped ZnO, the characteristic absorption peaks of RhB became weaker as the irradiation time increased, and disappeared almost completely after irradiation for 120 min (Figure 4a). Panels b and c in Figure 4 show that ZnO-core/SiO_2-shell composite nanoparticles had much lower efficiency to degrade RhB than PVP-capped ZnO nanoparticles. As the thickness of the shell increased, the reduction rate of the dye decreased. The ZnO-core/SiO_2-shell composite nanoparticles with the shell thickness of 25 nm showed only 8.7% intensity decrease of the UV/vis absorbance, which is similar to the intensity decrease of the absorption peak in the present of coreless SiO_2 nanoparticles with similar particle sizes (see Figure S1 in the Supporting Information). Thus the coating of SiO_2 on the surface of ZnO nanoparticles could markedly suppress the photodegradation of the RhB solution under the irradiation of simulated sunlight.

In this study, monodispersed ZnO-core/SiO_2-shell composite nanoparticles with high core loading levels were successfully prepared using a reverse microemulsion method. The aging time was shown to be a critical parameter in tuning the shell thickness between 11 and 25 nm. The photocatalytic activity of ZnO nanoparticles was greatly decreased by SiO_2 coating. The thicker SiO_2 shell resulted in less photoactivity. Consequently, reduced cytotoxicity could also be expected from the ZnO-core/SiO_2-shell composite nanoparticles, which is of particular importance for the use of ZnO in personal-care products. Further research on the application of ZnO-core/SiO_2-shell composite nanoparticles as an UV blocking agent is in progress.

Acknowledgment. This research is supported by the Central Research Grants Scheme at Deakin University, Australia.

Supporting Information Available: Detailed experimental regarding synthesis of PVP-capped ZnO and photocatalytic activity test, UV/vis spectrum of Rhodamine B degradation in the presence of SiO_2 nanoparticles (PDF). This material is available free of charge via the Internet at http://pubs.acs.org.

REFERENCES AND NOTES

(1) Yang, Y.; Gao, M. *Adv. Mater.* **2005**, *17*, 2354–2357.
(2) Jeong, U.; Teng, X.; Wang, Y.; Yang, H.; Xia, Y. *Adv. Mater.* **2007**, *19*, 33–60.
(3) Zhang, L.; Qiao, S.; Jin, Y.; Yang, H.; Budihartono, S.; Stahr, F.; Yan, Z.; Wang, X.; Hao, Z.; Lu, G. Q. *Adv. Funct. Mater.* **2008**, *18*, 3203–3212.
(4) Zhang, L.; Qiao, S. Z.; Jin, Y. G.; Chen, Z. G.; Gu, H. C.; Lu, G. Q. *Adv. Mater.* **2008**, *20*, 805–809.
(5) Li, L.; Choo, E. S. G.; Yi, J.; Ding, J.; Tang, X.; Xue, J. *Chem. Mater.* **2008**, *20*, 6292–6294.
(6) Yi, D. K.; Selvan, S. T.; Lee, S. S.; Papaefthymiou, G. C.; Kundaliya, D.; Ying, J. Y. *J. Am. Chem. Soc.* **2005**, *127*, 4990–4991.
(7) Zhang, Q.; Chou, T. P.; Russo, B.; Jenekhe, S. A.; Cao, G. *Angew. Chem., Int. Ed.* **2008**, *47*, 2402–2406.
(8) Law, J. B. K.; Thong, J. T. L. *Appl. Phys. Lett.* **2006**, *88*, 133113–113114.
(9) Kind, H.; Yan, H.; Messer, B.; Law, M.; Yang, P. *Adv. Mater.* **2002**, *14*, 158–160.
(10) Könenkamp, R.; Word, R. C.; Godinez, M. *Nano Lett.* **2005**, *5*, 2005–2008.
(11) Ramakrishna, G.; Ghosh, H. N. *Langmuir* **2003**, *19*, 3006–3012.
(12) Becheri, A.; Durr, M.; Nostr, P. L.; Baglioni, P. *J. Nanopart. Res.* **2008**, *10*, 679–689.
(13) Wang, R. H.; Xin, J. H.; Tao, X. M. *Inorg. Chem.* **2005**, *44*, 3926–3930.
(14) Sun, L.; Rippon, J. A.; Cookson, P.; Wang, X. G.; King, K.; Koulaeva, O.; Beltrame, R. *Int. J. Technol. Transfer Commerce* **2008**, *7*, 224–235.
(15) Dunford, R.; Salinaro, A.; Cai, L.; Serpone, N.; Horikoshi, S.; Hidaka, H.; Kownland, J. *FEBS Lett.* **1997**, *418*, 87–90.
(16) Selvan, S. T.; Tan, T. T.; Ying, J. Y. *Adv. Mater.* **2005**, *17*, 1620–1625.
(17) Lu, Y.; Yin, Y.; Mayers, B. T.; Xia, Y. *Nano Lett.* **2002**, *2*, 183–186.
(18) Bagwe, R. P.; Yang, C.; Hilliard, L. R.; Tan, W. *Langmuir* **2004**, *20*, 8336–8342.
(19) Haase, M.; Weller, H.; Henglein, A. *J. Phys. Chem. B* **1988**, *92*, 482–487.
(20) Guo, L.; Yang, S.; Yang, C.; Yu, P.; Wang, J.; Ge, W.; Wong, G. K. L. *Appl. Phys. Lett.* **2000**, *76*, 2901–2903.
(21) Yan, Q. Y.; Purkayastha, A.; Kim, T.; Kroger, R.; Bose, A.; Ramanath, G. *Adv. Mater.* **2006**, *18*, 2569–2573.
(22) Chen, S. L.; Dong, P.; Yang, G. H.; Yang, J. J. *J. Colloid Interface Sci.* **1996**, *180*, 237–241.
(23) Arriagada, F. J.; Osseo-Asare, K. *J. Colloid Interface Sci.* **1999**, *211*, 210–220.
(24) Graf, C.; Vossen, D. L. J.; Imhof, A.; Blaaderen, A. V. *Langmuir* **2003**, *19*, 6693–6700.

AM100051Z